

Microstructural stability and nanoindentation of an electrodeposited nanocrystalline Ni-1.5wt.%P alloy

M. J. N. V. Prasad*, A. H. Chokshi

Department of Materials Engineering, Indian Institute of Science, Bangalore 560 012, India

Received 21 July 2010, received in revised form 13 August 2010, accepted 20 August 2010

Abstract

Microstructural stability of nanocrystalline Ni-1.5wt.%P alloy with an initial grain size of 3 nm processed by pulsed electrodeposition was studied using differential scanning calorimetry (DSC) and annealing. Microstructural characterization suggests that the observed exothermic peak during heating in DSC is related to both concurrent grain growth and Ni₃P formation. Nanoindentation on samples with grain sizes from 3 to 50 nm revealed a breakdown in Hall-Petch strengthening in nano Ni-P alloy at grain sizes ≤ 10 nm, consistent with some previous observations. It is concluded that there is a grain boundary weakening regime for grain sizes < 10 nm, based on analysis which show that the data cannot be rationalized in terms of microstrain relaxation, variation in elastic modulus, texture evolution and duplex structure formation.

Key words: nanocrystalline, nickel, nanoindentation, Hall-Petch relationship, grain boundary weakening

1. Introduction

A reduction in grain size offers a convenient means for enhancing the strength of metals, as described by the well-known Hall-Petch relationship:

$$\sigma_y = \sigma_0 + k_y d^{-1/2}, \quad (1)$$

where σ_y is the yield stress for a material with a grain size of d , σ_0 is a friction stress and k_y is a constant. For hardness measurements, a similar equation is valid, with the slope being given by k_H ; for typical consideration of $H = 3 \sigma_y$, it follows that $k_H = 3k_y$. The above relationship suggests enormous increase in strength with a reduction in grain size from the conventional values of $> 10 \mu\text{m}$ to $< 100 \text{nm}$. Although there have been several reports of enhanced strength in nanocrystalline metals, there are also several reports of a grain boundary weakening regime at ultrafine grain sizes of less than $\sim 20 \text{nm}$ attributed to processes such as diffusion creep, grain boundary sliding and rotation [1–3].

Electrodeposition offers a simple and convenient means for producing dense nanocrystalline metals, either as free-standing films or as coatings. Conven-

tional direct current (dc) electroplating usually leads to a columnar grain structure whereas pulsed electrodeposition leads to an equiaxed grain morphology [4]. Nickel plating has been used for many decades for its hardness, which provides resistance to wear. It had also been known that the addition of P leads to additional hardness and concomitant wear resistance in Ni-P alloys [5, 6]. There have been several studies on nanocrystalline Ni and Ni-P alloys prepared by electrodeposition. The mechanical data suggest that the hardness of nano-Ni increases with a decrease in grain size down to $\sim 20 \text{nm}$; at much finer grain sizes, there are some reports of grain boundary weakening [7].

Electrodeposited nano-Ni is quite stable up to temperatures (T) $\sim 450 \text{K}$; there is evidence for extensive grain growth together with the formation of bimodal grain size distributions at higher temperatures [8]. In contrast to nano-Ni, where it is difficult to obtain grain sizes below $\sim 8 \text{nm}$, experiments reveal that it is possible to obtain much finer grain sizes down to $\sim 2 \text{nm}$ (and also amorphous metals) in nano Ni-P alloys [9]. Furthermore, the Ni-P alloys have a greater microstructural stability to temperatures up to $\sim 600 \text{K}$ due to either solute drag by P or a decrease in the grain

*Corresponding author: tel.: +91 80 2293 2684; e-mail address: prasad@materials.iisc.ernet.in

boundary energy caused by P segregation [10].

Mechanical tests on electrodeposited nano Ni-P alloys have demonstrated the occurrence of grain boundary softening for materials with grain sizes of < 10 nm [5, 6, 11–13]. The different grain sizes for the tests have been obtained by annealing very fine grained specimens, changing the electrodeposition parameters or altering the P content. Grain boundary weakening has been attributed to the larger contribution of triple junctions to deformation [12], the formation of Ni_3P precipitates during annealing to produce coarser grain sizes [5], and grain boundary relaxation and P segregation to grain boundaries [13]. There is evidence for considerable residual strains in electrodeposited Ni-P alloys, with the strains varying generally with P content and other deposition parameters [6]. Also, the texture in the as-deposited alloys can vary substantially with changes in the deposition parameters [5, 12]. It is therefore difficult to identify easily the causes for the observed grain boundary softening. Chang et al. [13] conducted an interesting study where attention was paid to residual strains in materials with different grain sizes and P content; however, they focused largely on grain sizes greater than ~ 10 nm, which is higher than the conventional softening regime, and they used dc plating instead of pulsed plating.

The present study was undertaken to evaluate the microstructural stability and strength of a nano Ni-P alloy, paying close attention to the possible influence on strength by the formation of Ni_3P particles, residual strains and texture.

2. Experimental material and procedure

Pulsed electrodeposition was used to produce a nanocrystalline Ni-P alloy. A modified Watts bath containing 300 grams per liter (gpl) nickel sulfate, 45 gpl nickel chloride and 45 gpl boric acid was used as the basic electrolyte, to which 30 gpl of phosphorous acid (H_3PO_3) was added as a P source. The electrolytic bath also contained about 2 gpl of saccharin as a stress reliever, and 0.4 gpl of sodium lauryl sulfate as a wetting agent. The bath temperature of 333 K and a pH of 1.2 were maintained during deposition. Titanium foil was used as a substrate and pure nickel as the soluble anodic material. A current density of 430 mA cm^{-2} was pulsed with an on-time of 5 ms and an off-time of 45 ms. Electrodeposition was carried out for 5 h to obtain foils with a nominal thickness of about 120 μm .

For thermal stability studies, nano Ni-P alloy samples of ~ 30 mg were heated at a rate of 10 K min^{-1} from 300 to 823 K in a differential scanning calorimetry (DSC). The calorimetric data for nano Ni-P alloy were generated at different heating rates (β) of 5, 10, 20 and 50 K min^{-1} for activation

energy measurements. In addition, samples were also annealed isothermally in a tubular furnace for different times. All samples were heated under a continuous circulation of ultra-high purity argon gas.

Nanoindentation measurements were performed at room temperature using a Berkovich indenter in a Hysitron triboindenter. A peak load of $500 \mu\text{N}$ was applied with a loading and unloading rate $50 \mu\text{N s}^{-1}$; about 10 measurements were taken for each condition. The hardness and modulus were calculated from the indentation load-penetration depth curves [14].

The phosphorous content in the as-deposited foil was determined using an electron microprobe. X-ray diffraction (XRD) measurements were performed using $\text{Cu K}\alpha$ radiation at a voltage of 40 kV and 30 mA in a Panalytical Xpert-pro XRD machine. The grain sizes and microstrains in the as-deposited foil and in the low temperature annealed samples were determined using the Warren-Averbach method (W-A) and the (111)-(222) peaks. Samples annealed at high temperatures, with coarser grain sizes, were examined by scanning electron microscopy (FEI-Sirion) after electropolishing in an electrolyte of 90 % ethanol + 10 % perchloric acid (voltage 20 V and temperature ~ 260 K); a linear intercept technique was used to characterize such grain sizes. The as-deposited sample and some selected annealed samples were characterized by transmission electron microscopy (FEI-Tecnai-F30) for the evolution of grain structure and second phase precipitation. TEM samples were prepared by ion-milling at a voltage of 5 kV in precision ion polishing system.

3. Experimental results

Electron microprobe analysis of the as-deposited films revealed a P content of 1.54 wt.%, and the alloy is therefore listed as Ni-1.5P.

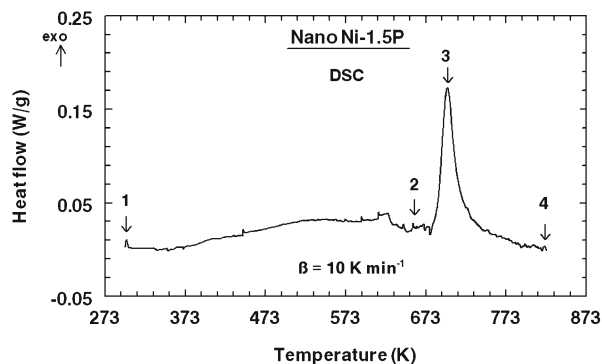


Fig. 1. DSC scan at a constant heating rate of 10 K min^{-1} for a nano Ni-1.5wt.%P alloy with an initial grain size of 3 nm; the arrows with numbers correspond to conditions for XRD characterization.

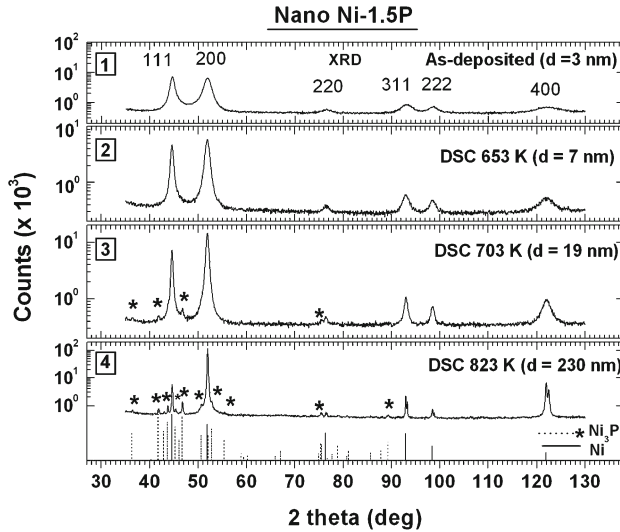


Fig. 2. XRD patterns of nano Ni-1.5wt.%P alloy samples in the as-deposited condition (location 1), and heated to different temperatures (locations at 2 to 4 shown in Fig. 1) in DSC at a heating rate of 10 K min^{-1} .

Figure 1 shows a DSC thermogram for an as-deposited sample obtained at a heating rate of 10 K min^{-1} ; the data depict a strong exothermic peak at 703 K , with an energy release of $\sim 20 \text{ J g}^{-1}$. It is clear also that there is a broad diffuse peak from 350 to 673 K before the strong exothermic peak. The XRD patterns of the samples heated to conditions labeled in Fig. 1 are illustrated in Fig. 2. Inspection of Fig. 2 reveals the initial grain size of 3 nm in the as-deposited condition grows to 230 nm at 823 K , with clear evidence for the presence of a Ni_3P phase at 703 K . Based on the intensities of the (200) peaks, the data also suggest a change in the texture following significant grain growth.

The activation energy (Q) associated with the strong exothermic reaction was calculated from Kissinger analysis [15], using the shift in the peak temperature (T_p) with heating rate, β :

$$\ln(\beta/T_p^2) = -(Q/RT_p) + \ln C, \quad (2)$$

where R is the gas constant and C is a constant. The current experimental data are shown in Fig. 3 in terms of the above analysis, yielding an activation energy of $\sim 200 \text{ kJ mol}^{-1}$. This value is consistent with previous reports in other Ni-P alloys [10, 16], but substantially different from the values of ~ 120 and 290 kJ mol^{-1} for grain boundary and lattice diffusion, respectively, in Ni [17].

Figure 4 shows the variation in grain size and microstrain for samples annealed for 30 minutes at various temperatures. It is clear that the initial large microstrain of $\sim 0.4 \%$ is reduced substantially to

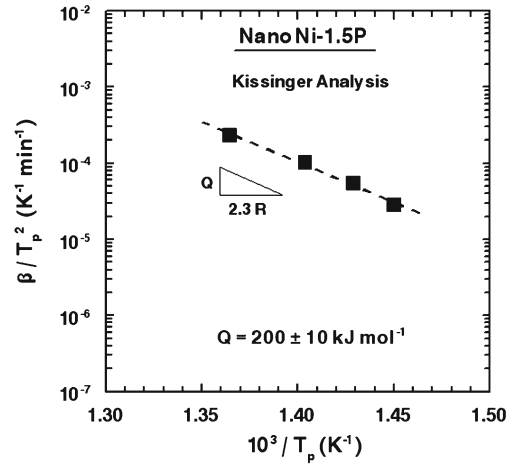


Fig. 3. Kissinger plot for the exothermic peak observed for nano Ni-1.5wt.%P alloy during heating at different constant heating rates in DSC.

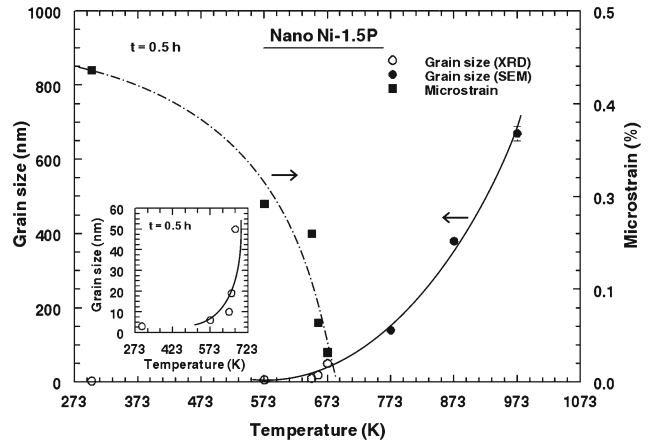


Fig. 4. Grain size and microstrain data of nano Ni-1.5wt.%P alloy annealed for 0.5 h at different temperatures; the inset is for the grain size evolution at low temperatures.

$\sim 0.2 \%$ at 623 K and $\sim 0.04 \%$ at 673 K ; it was not possible to measure microstrains or grain sizes by XRD in samples with coarse grain sizes. The grain sizes remained $\leq 50 \text{ nm}$ for annealing at $T < 673 \text{ K}$. Samples with grain sizes $\geq 19 \text{ nm}$ displayed additional XRD peaks corresponding to the Ni_3P phase.

Electron micrographs depicting the microstructural evolution during annealing are shown in Fig. 5 for (a) the as-deposited condition, and those annealed at (b) to (d) 648 , 773 and 973 K , respectively. No second phase particles could be detected in samples with grain sizes up to 10 nm (Figs. 5a,b), but particles could be detected in samples with grain sizes $\geq 19 \text{ nm}$ (Figs. 5c,d). It is clear that the Ni_3P phase size also increased with an increase in the Ni grain size. Image

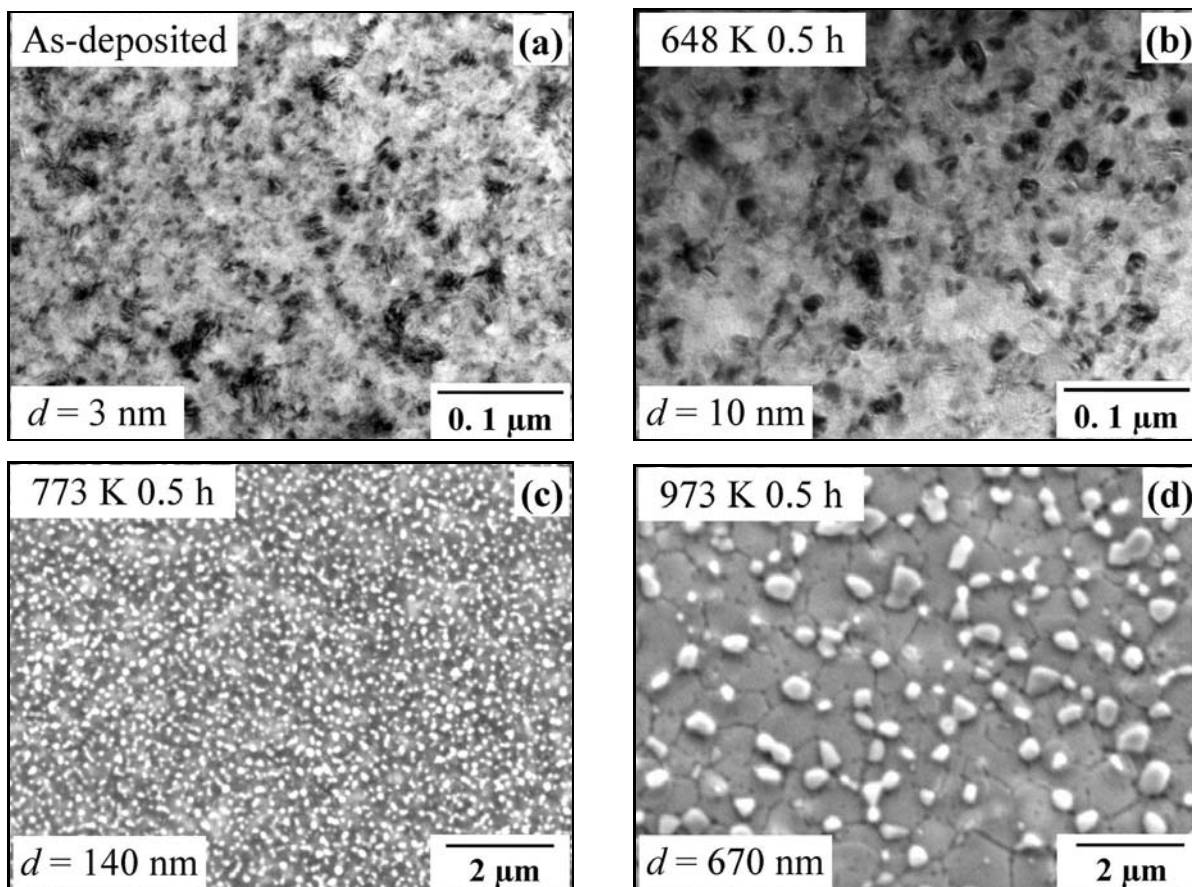


Fig. 5. TEM bright field images for nano Ni-1.5wt.%P alloy in (a) the as-deposited condition and annealed for 0.5 h at (b) 648 K, and SEM images for samples annealed at (c) 773 K and (d) 973 K.

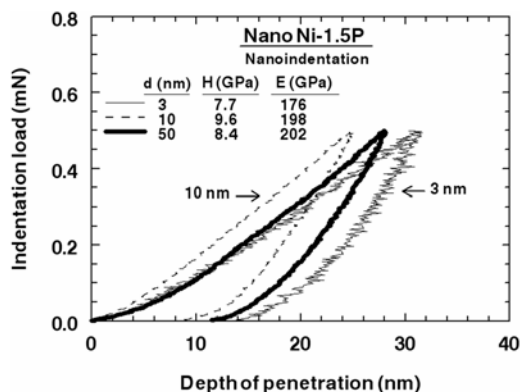


Fig. 6. Nanoindentation load vs penetration depth curves for nano Ni-1.5wt.%P alloy with three different grain sizes.

analysis of samples with coarse grain sizes revealed a second phase area fraction of $12 \pm 1\%$, compared with a theoretical value of $\sim 15\%$ based on the chemical composition of the alloy; the difference is attributed to the presence of fine intragranular precipitates that were not included in the image analysis.

Figure 6 illustrates the indentation load-penetration ($P-h$) curves from nanoindentation experiments

under three different experimental conditions. All of the experimental results are summarized in Table 1 in terms of the processing condition, grain size, microstrain, and the elastic modulus and hardness evaluated from nanoindentation experiments. The as-deposited condition ($d = 3$ nm) led to a larger microstrain and somewhat lower values of the elastic modulus and hardness. Samples with grain sizes of 6 and 10 nm were single phase and had a similar value of residual strain, Young's modulus and hardness. At the coarsest grain size of 50 nm, the microstructure was no longer single phase.

4. Discussion

Microstructural evolution. Since the phase diagram indicates that there is very little solubility of P in Ni [18], it is clear that the as-deposited nano Ni-1.5P alloy is in a metastable condition; it is anticipated that Ni_3P phase particles will eventually form during annealing. The present experimental study revealed that the alloy remained in a single phase condition for grain sizes of ≤ 10 nm. Although the sequence of precipitation was not followed, it is anticipated that

Table 1. Nanoindentation data for nano Ni-1.5P alloy

Condition	XRD-grain size (nm)	Microstrain (%)	Elastic modulus (GPa)	Hardness (GPa)
As-deposited	3	0.43	176 ± 10	7.7 ± 0.4
573 K 0.5 h	6	0.24	198 ± 5	9.4 ± 0.4
648 K 0.5 h	10	0.20	198 ± 8	9.6 ± 0.5
673 K 0.5 h	50	0.04	202 ± 10	8.4 ± 0.4

P will segregate to grain boundaries during annealing and that Ni₃P particles will form upon reaching a critical concentration of P at grain boundaries. Calculations suggest that a monolayer coverage of P at grain boundaries will occur at a grain size of ~ 20 nm, and this is broadly consistent with the observations of second phase particles only in materials with grain sizes ≥ 19 nm.

The driving force for grain growth is expected to be proportional to (γ/d) , where γ is the grain boundary energy; a very fine grain size of 3 nm is likely to provide a large driving force for grain growth. The broad diffuse exotherm observed in DSC at $T \sim 320$ to 650 K is related to an increase in grain size from ~ 3 to 10 nm together with a decrease in γ related to progressive segregation of P [19]. Calculations show that the observed energy release of -20 J g^{-1} cannot be accounted for completely by grain growth and a reduction in residual strain. Therefore, as observed in a recent study on Ni-S [20], the exothermic peak is attributed to contributions from both grain growth and second phase formation. Clearly, in such a case, it is not possible to attribute the observed activation energy of ~ 200 kJ mol⁻¹ for the exothermic peak solely to grain growth or second phase formation.

The as-deposited nano Ni-1.5P exhibits a <111> texture, which changes gradually upon annealing to <100> texture after second phase formation; there was very little change in texture in materials with grain sizes of ≤ 10 nm. Experiments on nano-Ni have revealed a transition in texture from <100> to <111>, and this has been attributed to a minimization in the energy [21]. In the present alloy, the formation of Ni₃P phase and concomitant interphase boundaries add to the complexity in analyzing energy minimization.

Strength. The current experimental data on hardness are shown in Fig. 7 together with other sets of data on electrodeposited nano Ni-P alloys, in terms of the conventional Hall-Petch linear plot of the variation in hardness with $d^{-1/2}$. In addition to the present experimental results (filled inverted triangles), the figure also shows data from Palumbo et al. [11], Zhou et al. [12], Jeong et al. [5], Kobayashi and Kashikura [22], Hou et al. [6] and Chang et al. [13]; dashed lines in the lower left corner are based on an extrapolation of the Hall-Petch relationship for coarse grained Ni [23,

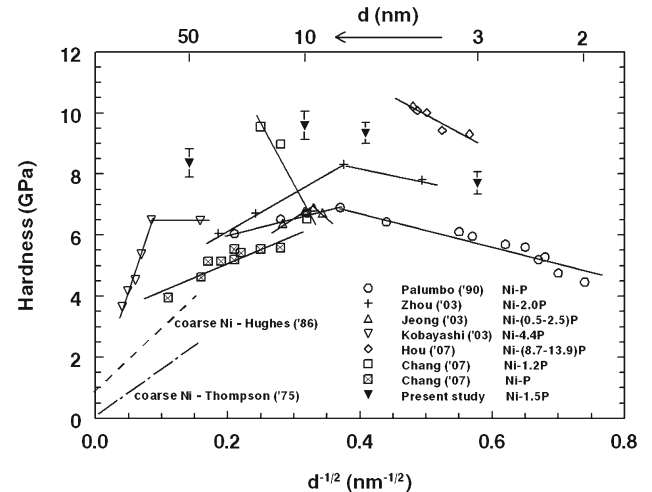


Fig. 7. Hall-Petch plot for comparison of the present experimental hardness data with previous experimental observations in electrodeposited nano Ni-P alloys.

24]. Unfortunately, many of the original publications do not give complete information on the compositions and procedures used to develop a range of grain sizes. The data reported by Kobayashi and Kashikura [22] involved materials with second phase Ni₃P particles, and these are not considered further in the discussion. Chang et al. [13] obtained a range of single phase Ni-P materials with fine grain sizes of ~ 12 to 60 nm with a similar residual strain, by changing the deposition conditions, and this revealed a positive Hall-Petch slope, indicative of grain boundary strengthening; however, the authors did not consider possible changes in texture, and their data were limited to grain sizes of > 10 nm.

It is clear that there are three additional sets of data indicating grain boundary softening at very fine grain sizes of ≤ 10 nm. There are at least four possible reasons for an apparent regime of grain boundary softening with decreasing grain size: (a) variation in elastic modulus, (b) change in texture, (c) development of a duplex microstructure, and (d) relaxation of residual strains by annealing to obtain different grain sizes. In the present study, there was no evidence for a change in texture or a development of duplex structures in materials with grain sizes ≤ 10 nm. There was

a slight decrease in the elastic modulus, and the residual strain was higher, in the as-deposited condition, compared to the other two datum points with grain sizes of 6 and 10 nm. However, for grain sizes of 6 and 10 nm, the residual strains and elastic modulus were similar, so that these data cannot be rationalized in terms of the four causes noted above.

Within experimental error, there was no significant change in the hardness for specimens with grain sizes of 10 and 6 nm, with hardness values of 9.6 and 9.4 GPa, respectively. Values for the Hall-Petch slope k_H range from ~ 15 to $21 \text{ GPa nm}^{-1/2}$ for Ni and $10.4 \text{ GPa nm}^{-1/2}$ for the single phase Ni-P data reported by Chang et al. [13]. Calculations using the standard Hall-Petch relation (Eq. (1)) with a hardness of 9.6 GPa at a grain size of 10 nm predict values of hardness of ~ 10.5 and 11.4 GPa for a grain size of 6 nm, for respective k_H values of 10 and $20 \text{ GPa nm}^{-1/2}$; the predicted values are much higher than the experimental value of 9.4 GPa for a grain size of 6 nm. The above analysis demonstrates clearly that the conventional Hall-Petch relationship for materials with grain sizes of $> 10 \text{ nm}$ is not valid at finer grain sizes.

The present experimental observations of a breakdown in Hall-Petch strengthening at very fine grain sizes are consistent with the many analyses showing difficulty in the operation of conventional dislocation processes for grain sizes of less than ~ 10 to 15 nm [25]. Grain boundary related processes are likely to become important for grain sizes of $\leq 10 \text{ nm}$, and although the details are not clear, processes such as grain boundary sliding and Coble creep may be relevant at these fine grain sizes. Since the data at the finest grain size of 3 nm involved a variation in both internal strain as well as Young's modulus, it is not possible to conclude from the present study that there is a regime with a negative Hall-Petch relation although it is clear that the conventional Hall-Petch strengthening process is not valid at grain sizes of $\leq 10 \text{ nm}$. It is interesting to note that Trelewicz and Schuh [26] suggested that the hardness essentially reaches a peak and does not change at fine grain sizes $< 10 \text{ nm}$, based on some data in a Ni-W alloy. It is important to note that deformation in the grain boundary weakening regime does not always lead to large ductility at room temperature due possibly to the high flow stresses and an inability of grain boundaries to act as perfect sources and sinks for defects; however, extraordinary superplasticity is possible at higher temperatures with grain sizes $\leq 500 \text{ nm}$ [27, 28].

The present experimental results show also that annealing an as-deposited alloy to change the grain size from 3 to 6 nm leads to a significant increase in strength; such observations of an increase in strength by annealing have been attributed generally to a decrease in residual strains and the corresponding increase in difficulty for dislocation nucleation at grain

boundaries. However, in the present study, it is not possible to establish conclusively the cause for the observed increase in hardness with annealing since the grain size, residual strain and Young's modulus are all altered by annealing.

5. Summary and conclusions

Pulsed electrodeposition was used to produce a single phase nano Ni-1.5wt.%P alloy with an initial grain size of 3 nm. An exothermic peak was noted at a temperature of $\sim 700 \text{ K}$ upon constant heating rate tests in a differential scanning calorimeter. Microstructural examination by XRD and electron microscopy revealed that the exothermic peak corresponded to Ni_3P compound formation together with grain growth. There was a significant change in texture with heat treatment, associated with the formation of a second phase. Nanoindentation experiments displayed a breakdown in Hall-Petch strengthening at grain sizes $\leq 10 \text{ nm}$, which cannot be interpreted in terms of changes in the elastic modulus, texture or residual strains. The breakdown in the Hall-Petch relationship is attributed to the difficulty in operation of conventional dislocation processes and the advent of grain boundary related processes.

Acknowledgements

We are grateful to the IISc nanoscience initiative for the use of electron microscopy facilities. This work was supported by the Department of Science and Technology.

References

- [1] CHOKSHI, A. H.—ROSEN, A.—KARCH, J.—GLEITER, H.: *Scripta Metall.*, 23, 1989, p. 1679. [doi:10.1016/0036-9748\(89\)90342-6](https://doi.org/10.1016/0036-9748(89)90342-6)
- [2] SCHIOTZ, J.—DI TOLLA, F. D.—JACOBSEN, K. W.: *Nature*, 391, 1998, p. 561. [doi:10.1038/35328](https://doi.org/10.1038/35328)
- [3] SHAN, Z.—STACH, E. A.—WIEZOREK, J. M. K.—KNAPP, J. A.—FOLLSTAEDT, D. M.—MAO, S. X.: *Science*, 305, 2004, p. 654. [doi:10.1126/science.1098741](https://doi.org/10.1126/science.1098741) PMID:15286368
- [4] BICELLI, L. P.—BOZZINI, B.—MELE, C.—D'URZO, L.: *Intern. J. Electrochem. Sci.*, 3, 2008, p. 356.
- [5] JEONG, D. H.—ERB, U.—AUST, K. T.—PALUMBO, G.: *Scripta Mater.*, 48, 2003, p. 1067. [doi:10.1016/S1359-6462\(02\)00633-4](https://doi.org/10.1016/S1359-6462(02)00633-4)
- [6] HOU, K. H.—JENG, M. C.—GER, M. D.: *J. Alloys Compd.*, 437, 2007, p. 289. [doi:10.1016/j.jallcom.2006.07.120](https://doi.org/10.1016/j.jallcom.2006.07.120)
- [7] PHANIRAJ, M. P.—PRASAD, M. J. N. V.—CHOKSHI, A. H.: *Mater. Sci. Eng. A*, 463, 2007, p. 231. [doi:10.1016/j.msea.2006.08.116](https://doi.org/10.1016/j.msea.2006.08.116)
- [8] PRASAD, M. J. N. V.—SUWAS, S.—CHOKSHI, A. H.: *Mater. Sci. Eng. A*, 503, 2009, p. 86. [doi:10.1016/j.msea.2008.01.099](https://doi.org/10.1016/j.msea.2008.01.099)

- [9] BREDAEL, E.—BLANPAIN, B.—CELIS, J. P.—ROOS, J. R.: *J. Electrochem. Soc.*, 141, 1994, p. 294. [doi:10.1149/1.2054703](https://doi.org/10.1149/1.2054703)
- [10] MEHTA, S. C.—SMITH, D. A.—ERB, U.: *Mater. Sci. Eng. A*, 204, 1995, p. 227. [doi:10.1016/0921-5093\(95\)09966-2](https://doi.org/10.1016/0921-5093(95)09966-2)
- [11] PALUMBO, G.—ERB, U.—AUST, K. T.: *Scripta Metall. Mater.*, 24, 1990, p. 2347.
- [12] ZHOU, Y.—ERB, U.—AUST, K. T.—PALUMBO, G.: *Scripta Mater.*, 48, 2003, p. 825. [doi:10.1016/S1359-6462\(02\)00511-0](https://doi.org/10.1016/S1359-6462(02)00511-0)
- [13] CHANG, L.—KAO, P. W.—CHEN, C. H.: *Scripta Mater.*, 56, 2007, p. 713. [doi:10.1016/j.scriptamat.2006.12.036](https://doi.org/10.1016/j.scriptamat.2006.12.036)
- [14] OLIVER, W. C.—PHARR, G. M.: *J. Mater. Res.*, 7, 1992, p. 1564. [doi:10.1557/JMR.1992.1564](https://doi.org/10.1557/JMR.1992.1564)
- [15] KISSINGER, H. E.: *J. Res. National Bur. Std.*, 57, 1956, p. 217.
- [16] LU, K.: *Nanostruct. Mater.*, 2, 1993, p. 643.
- [17] FROST, H. J.—ASHBY, M. F.: *Deformation Mechanism Maps*. Oxford, Pergamon Press 1982, p. 21.
- [18] MASSALSKI, T. B.—OKAMOTO, H.—SUBRAMANIAN, P. R.—KACPRZAK, L.: *Binary alloy phase diagrams*. Ed. 2. USA, ASM International 1990, p. 2835.
- [19] CHEN, Z.—LIU, F.—WANG, H. F.—YANG, W.—YANG, G. C.—ZHOU, Y. H.: *Acta Mater.*, 57, 2009, p. 1466. [doi:10.1016/j.actamat.2008.11.025](https://doi.org/10.1016/j.actamat.2008.11.025)
- [20] PRASAD, M. J. N. V.—CHOKSHI, A. H.: *Scripta Mater.*, 2010 (in press). [doi:10.1016/j.scriptamat.2010.11.038](https://doi.org/10.1016/j.scriptamat.2010.11.038)
- [21] KLEMENT, U.—SILVA, M. D.: *J. Alloys Compd.*, 434–435, 2007, p. 714. [doi:10.1016/j.jallcom.2006.08.118](https://doi.org/10.1016/j.jallcom.2006.08.118)
- [22] KOBAYASHI, S.—KASHIKURA, Y.: *Mater. Sci. Eng. A*, 358, 2003, p. 76. [doi:10.1016/S0921-5093\(03\)00285-5](https://doi.org/10.1016/S0921-5093(03)00285-5)
- [23] THOMPSON, A. A. W.: *Acta Metall.*, 23, 1975, p. 1337. [doi:10.1016/0001-6160\(75\)90142-X](https://doi.org/10.1016/0001-6160(75)90142-X)
- [24] HUGHES, G. D.—SMITH, S. D.—PANDE, C. S.—JOHNSON, H. R.—ARMSTRONG, R. W.: *Scripta Metall.*, 20, 1986, p. 93. [doi:10.1016/0036-9748\(86\)90219-X](https://doi.org/10.1016/0036-9748(86)90219-X)
- [25] KUMAR, K. S.—VAN SWYGENHOVEN, H.—SURESH, S.: *Acta Mater.*, 51, 2003, p. 5743. [doi:10.1016/j.actamat.2003.08.032](https://doi.org/10.1016/j.actamat.2003.08.032)
- [26] TRELEWICZ, J. R.—SCHUH, C. A.: *Acta Mater.*, 55, 2007, p. 5948. [doi:10.1016/j.actamat.2007.07.020](https://doi.org/10.1016/j.actamat.2007.07.020)
- [27] PRASAD, M. J. N. V.—CHOKSHI, A. H.: *Scripta Mater.*, 63, 2010, p. 136. [doi:10.1016/j.scriptamat.2010.03.034](https://doi.org/10.1016/j.scriptamat.2010.03.034)
- [28] PRASAD, M. J. N. V.—CHOKSHI, A. H.: *Acta Mater.*, 58, 2010, p. 5724. [doi:10.1016/j.actamat.2010.06.047](https://doi.org/10.1016/j.actamat.2010.06.047)